Cell Reports, Volume *40*

Supplemental information

Limbal BCAM expression identifies a proliferative progenitor population capable of holoclone formation and corneal differentiation

Yuzuru Sasamoto, Catherine A.A. Lee, Brian J. Wilson, Florian Buerger, Gabrielle Martin, Ananda Mishra, Shoko Kiritoshi, Johnathan Tran, Gabriel Gonzalez, Friedhelm Hildebrandt, Vickie Y. Jo, Christine G. Lian, George F. Murphy, Bruce R. Ksander, Markus H. Frank, and Natasha Y. Frank

Supplementary Figures

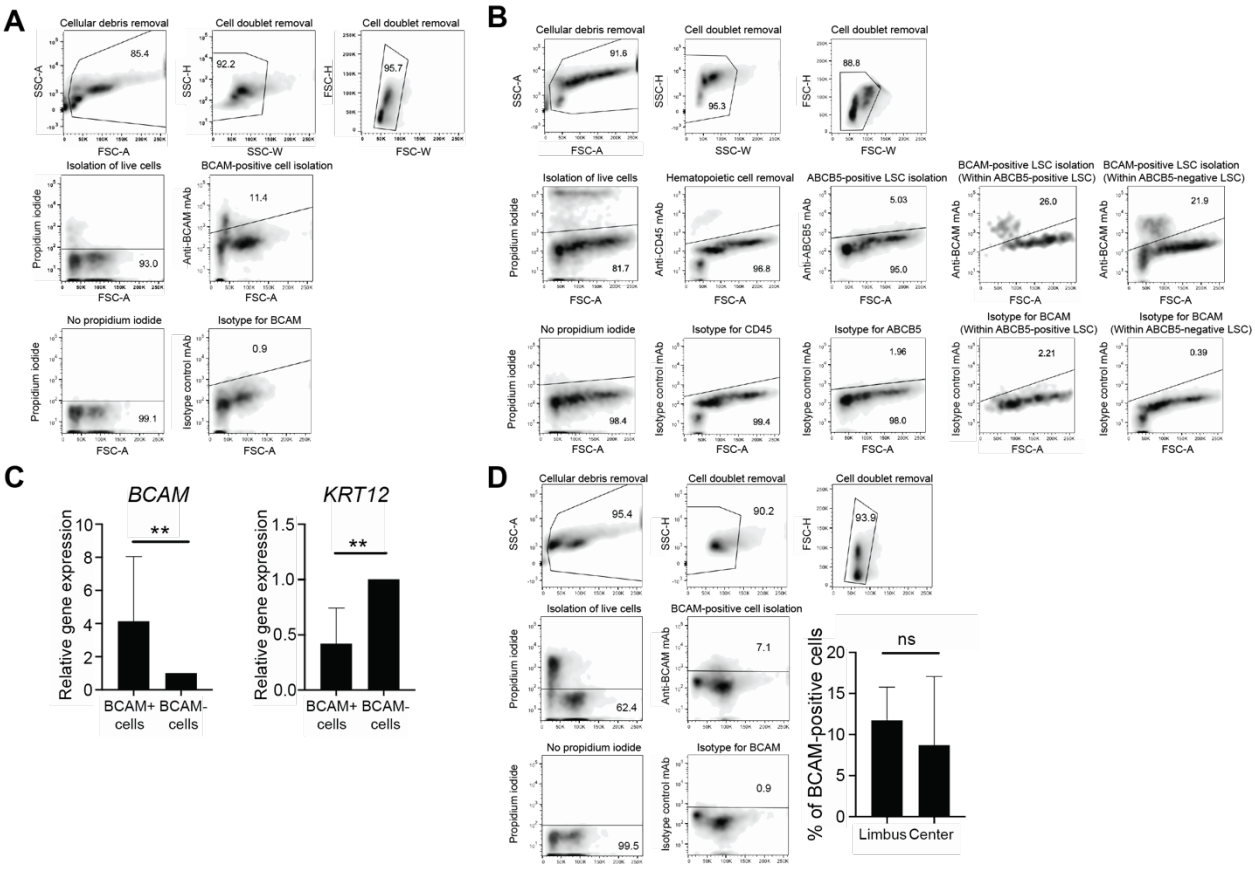

Figure S1. Characterization of BCAM-positive cells in limbus and central cornea. Related to Figure 1.

(**A**), Representative flow cytometric analyses of BCAM expression in limbal epithelial cells. FSC, forward scatter; SSC, side scatter; A, area; W, width; H, height.

(**B**), Representative flow cytometric analyses depicting BCAM expression in ABCB5-positive LSCs. FSC, forward scatter; SSC, side scatter; A, area; W, width; H, height.

(**C**), Bar graphs represent *BCAM* and *KRT12* expression in limbal BCAM-positive and BCAM-negative cells (mean±SD; n= 8; **p < 0.01, ns: not significant). Data were analyzed using a Wilcoxon matched-pairs signed rank test.

(**D**), Representative flow cytometric analyses of BCAM expression in central corneal epithelial cells. The bar graph depicts the percentage of BCAM-positive cells in the limbus and central cornea (mean±SD; n=11; ns: not significant). Data were analyzed using a paired t-test. FSC, forward scatter; SSC, side scatter; A, area; W, width; H, height.

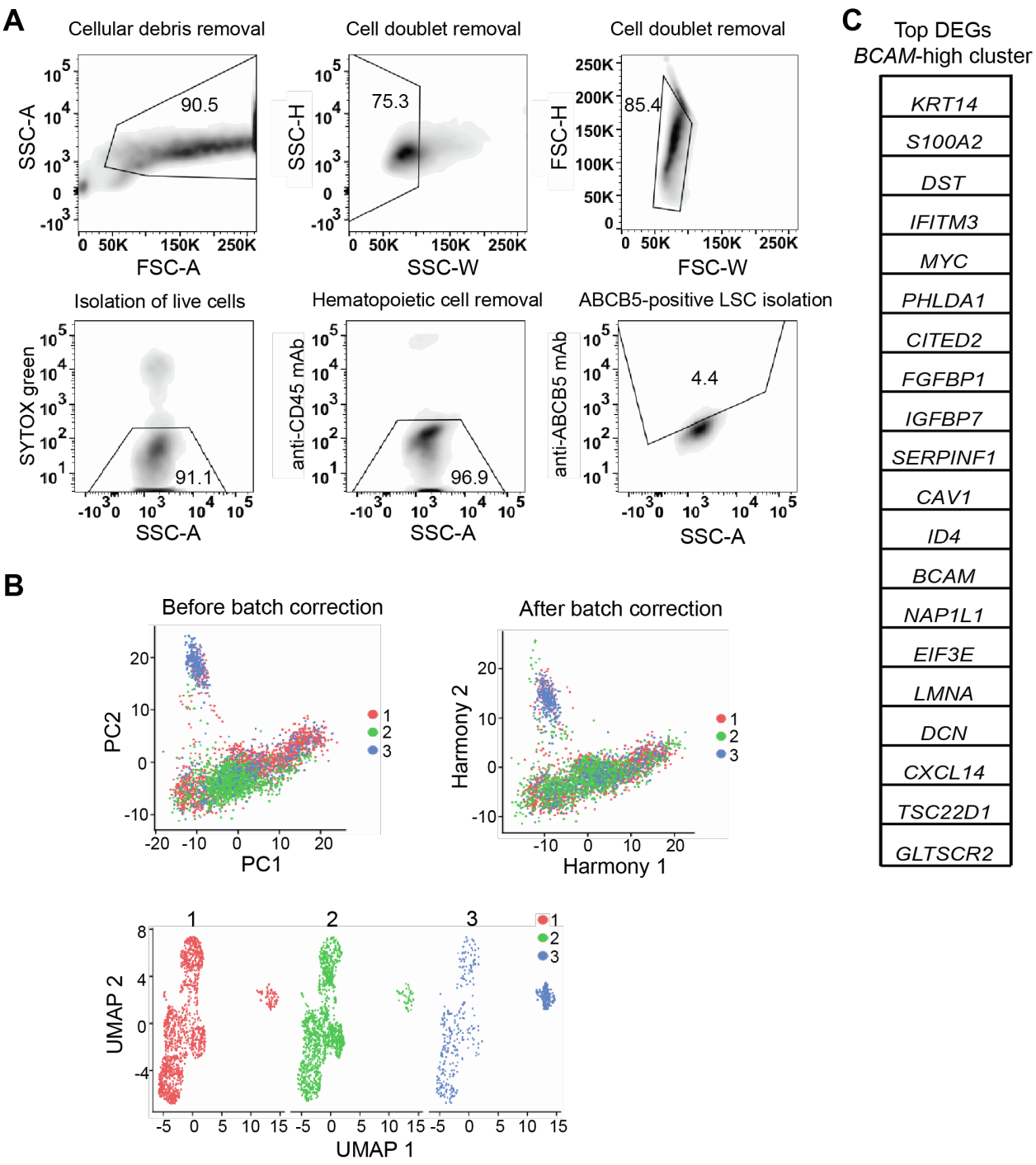

Figure S2. Isolation and scRNA-seq analyses of ABCB5-positive LSCs from three human donors. Related to Figure 2.

(**A**) Representative flow cytometric analyses employed for the isolation of ABCB5-positive LSCs. FSC, forward scatter; SSC, side scatter; A, area; W, width; H, height. (**B**) UMAP of Seurat clustering before batch correction (upper panel) and after batch correction (middle panel) with Harmony. UMAP of Seurat clustering after batch

correction shown for each sample (lower panel). Each color represents an individual patient (n = 3).
(**C**) List of the top 20 differentially expressed genes enriched in the *BCAM*-high cluster compared to the *BCAM*-low cluster.

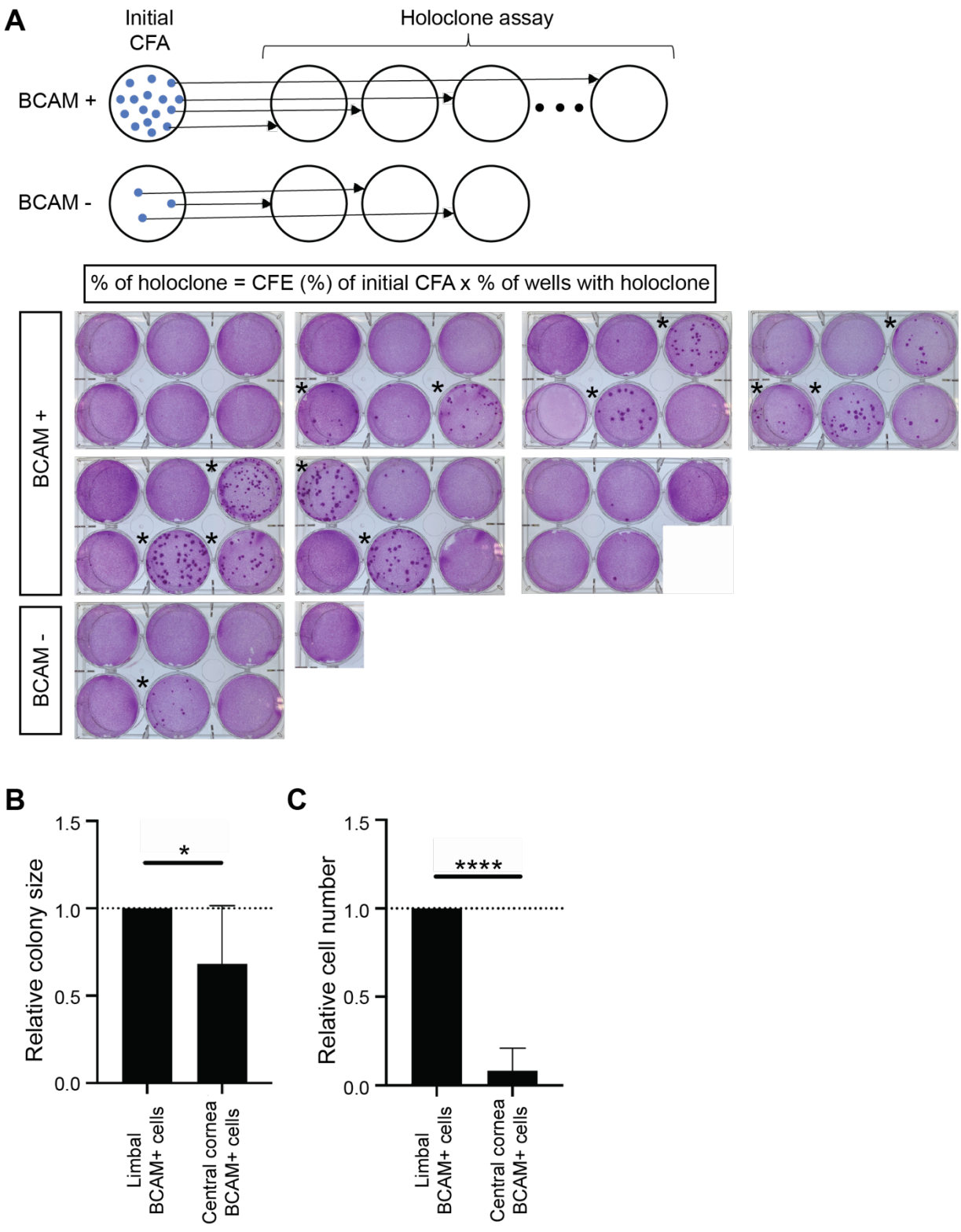

Figure S3. Superior proliferation potential of limbal BCAM-positive cells. Related to Figure 3.

(A) Schematic illustration of the holoclone assay (upper panel). Colonies were picked up from the initial colony-forming assay (CFA), dissociated, and seeded onto the new wells. The percentage of holoclones is calculated by multiplying the colony-forming efficiency (CFE) (%) of initial CFA by the percentage of wells containing a holoclone among the seeded wells. Representative macroscopic images of the wells with holoclones generated by limbal BCAM-positive and BCAM-negative cells are shown in the lower panel. Individual colonies are stained with Rhodamine B (pink). CFE; colony-forming efficiency, CFA; colony-forming assay. *Holoclone.
(**B**), Bar graph represents the relative colony size of BCAM-positive cells in the limbus and central cornea (mean±SD; n = 7, *$p < 0.05$). Data were analyzed using a paired t-test.
(**C**), Bar graph shows relative cell numbers of cultured BCAM-positive cells in the limbus and central cornea (mean±SD; n = 5; ****$p < 0.0001$). Data were analyzed using a paired t-test.

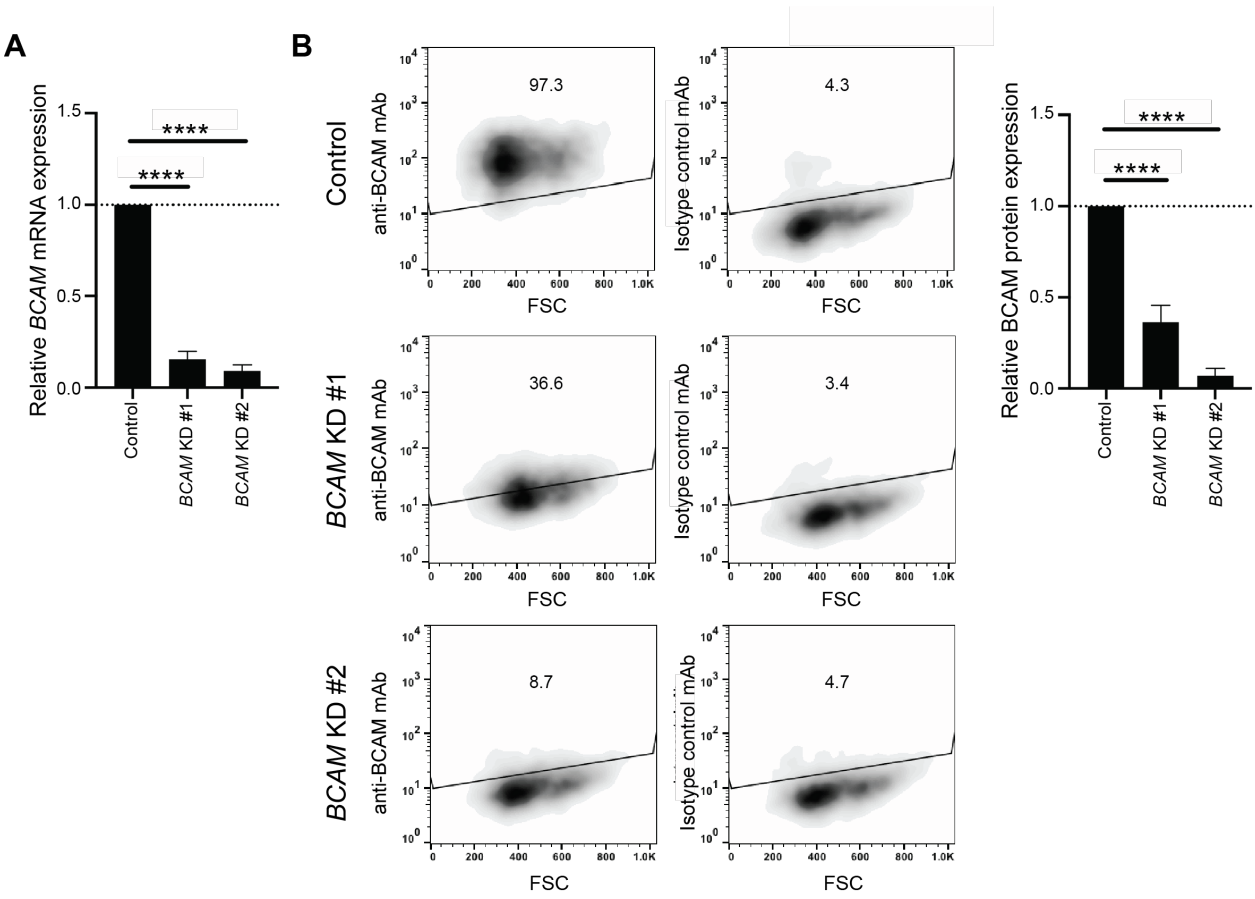

Figure S4. siRNA-induced BCAM blockade in limbal epithelial cells. Related to Figure 5.

(**A**) Bar graph depicts *BCAM* mRNA expression in control and *BCAM* siRNA-treated limbal epithelial cells (mean±SD; n = 8; ****p < 0.0001). Data were analyzed using a Dunnett's multiple comparisons test.

(**B**) Left, representative flow cytometric analysis of BCAM expression in control and *BCAM* siRNA-treated cells limbal epithelial cells. Right, bar graph represents relative percentage of BCAM-positive cells (mean±SD; n = 10; ****p < 0.0001). KD, knockdown. Data were analyzed using a Dunnett's multiple comparisons test.

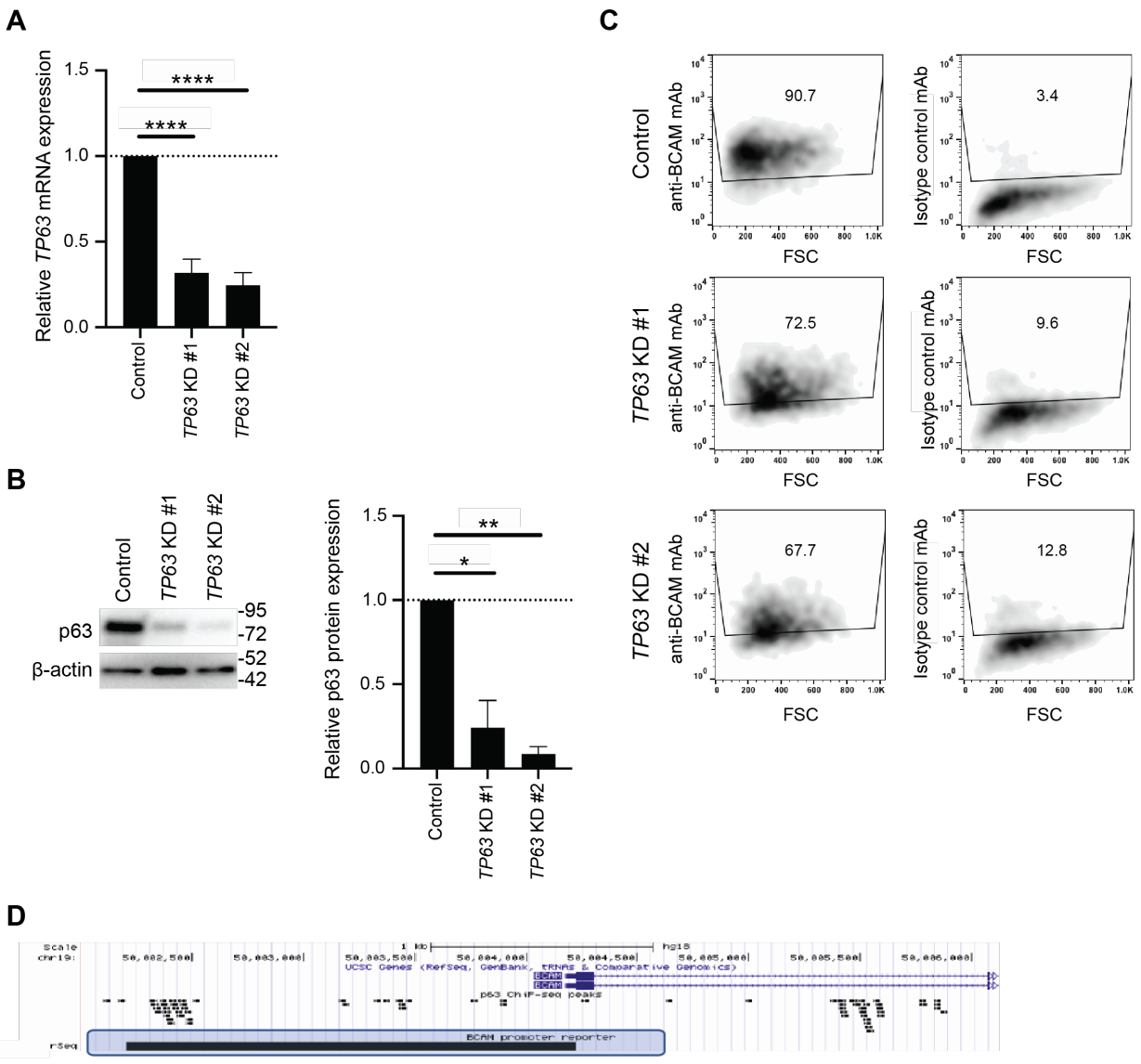

Figure S5. siRNA-induced p63 blockade attenuates BCAM expression in limbal epithelial cells. Related to Figure 6.

(**A**) Bar graph depicts *TP63* mRNA expression in control and *TP63* siRNA-treated limbal epithelial cells (mean±SD; n = 8; ****p < 0.001). Data were analyzed using a Dunnett's multiple comparisons test. KD, knockdown.

(**B**) Left, Western blot analyses of p63 expression in control and *TP63* siRNA-treated limbal epithelial cells. Right, bar graph represents the quantitative analyses of p63 protein expression (mean±SD; n = 3; *p < 0.05, p** < 0.01). Data were analyzed using a Dunnett's multiple comparisons test.

(**C**), Representative flow cytometric analyses of BCAM expression in control and *TP63* siRNA-treated limbal epithelial cells.

(**D**) The graph illustrates the position of the *BCAM* promoter sequence used for the luciferase reporter construct visualized using the UCSC genome browser.

Table S1. Donor characteristics for corneas used for single cell RNA-seq analyses and respective figures. Related to Figure 2.

#	Age	Gender	Smoking	Cause of death	Figures
1	28	Male	-	Acute respiratory distress syndrome caused by silicone injection syndrome	Figures 2, S2, and 4A
2	59	Male	-	Acute Cardiac Event	Figures 2, S2, and 4A
3	46	Male	-	Subarachnoid hemorrhage	Figures 2, S2, and 4A

Table S2. Donor characteristics for corneas used in validation analyses and respective figures. Related to Figures 1,3,4,5,6

#	Age	Gender	Smoking	Cause of death	Figures
1	35	Male	-	Overdose	Figures 1G, 1H, 1I, 4B and 6A
2	62	Male	-	Lymphoma	Figures 1G, 1H, 1I, 4B and 6A
3	58	Male	-	Probable hypertensive cardiovascular disease	Figures 1G, 1H, 1I, 4B and 6A
4	65	Male	-	End stage renal disease	Figures 6B, S4A and S5A
5	74	Male	+	Cardiac event	Figures 6B, S4A and S5A
6	56	Male	+	Subarachnoid hemorrhage	Figures 5B, 6B, 6C, S4A, S4B, S5A and S5B
7	64	Female	-	Cancer	Figures 5B, 6B, 6C, S4A, S4B, S5A, S5B and S5C
8	65	Male	+	Cancer	Figures 5B, 6B, 6C, S4A, S4B and S5A
9	75	Male	+	Acute cardiac event	Figures 5B, 6B, 6C, S4A, S4B, S5A and 6E
10	70	Male	-	End stage renal disease	Figures 5B, 6B, 6C, S4A, S4B, S5A, S5B and 6E
11	50	Female	-	Acute cardiac event	Figures 4C, 5B, and S4B
12	66	Female	+	Acute cardiac event	Figures 5B, S4A, S4B and 6E
13	63	Female	+	Acute cardiac event	Figures 4C, 5B, 6B, 6C, S4B and S5A
14	73	Male	-	Acute cardiac event	Figures 4C and S4B
15	20	Female	-	Anoxic brain injury	Figures 5C and 6E
16	64	Female	+	Anoxic brain injury	Figure 5C
17	75	Female	+	Cancer	Figures 3D and 5C

18	70	Male	+	Acute cardiac event	Figure 5C
19	55	Male	+	Cancer	Figure 5C
20	59	Male	-	Acute cardiac event	Figures 3D, 5A and 5C
21	48	Male	+	Cancer	Figure 5C
22	75	Male	+	Acute cardiac event	Figures 3D and 3E
23	58	Male	+	Congestive Heart Failure	Figures 3D, 3E, 5A and S1D
24	55	Male	+	Cancer	Figures 3D, 3E and 5A
25	65	Male	+	Cancer	Figures 3D, 3E and 5A
26	61	Male	+	Acute cardiac event	Figure 3D
27	34	Male	+	Acute cardiac event	Figure 5A
28	59	Female	+	Acute cardiac event	Figure 5A
29	72	Female	+	Acute cardiac event	Figure 5A
30	78	Female	-	Respiratory	Figures 3A, 3B, 3C, S1D, S3B and S3C
31	78	Female	+	Myocardial infarction	Figure S1A
32	19	Male	-	Anoxic brain injury	Figure S1D
33	72	Female	+	Myocardial infarction	Figure 6E
34	74	Male	+	Acute cardiac event	Figures S4B and 6E
35	77	Female	+	Chronic obstructive pulmonary disease	Figure 3A
36	78	Female	-	Acute cardiac event	Figures 3A and S1C
37	55	Male	+	Sepsis	Figures 3A, 3B and S1C
38	79	Male	+	End stage renal disease	Figure S1C
39	71	Female	-	Acute respiratory failure	Figures 3A and 3B
40	64	Female	-	Cancer	Figures 3A, 3B, S1C and S1D
41	75	Female	-	End stage renal disease	Figures 3A, 3B, 3C, S1C, S1D, S3B and S3C
42	70	Female	+	Respiratory failure	Figures 3A, 3B, 3C, S1C, S1D, S3A, S3B and S3C
43	77	Male	-	Acute cardiac event	Figure S1D
44	74	Female	-	Gastrointestinal bleeding	Figures 3A, 3C, S1D, S3B and S3C
45	77	Female	-	Cerebrovascular accident	Figures 3A, 3B, 3C, S1C, S1D, S3B and S3C
46	69	Female	+	Sepsis	Figures 3A, 3C, S1C, S1D and S3B
47	66	Female	+	Multi-system failure	Figures 3A, 3C, S1D and S3B
48	63	Female	+	Myocardial infarction	Figures 1C, 1D, 1E and 1F
49	64	Female	-	Acute cardiac event	Figures 1C, 1E, 1F and S1B
50	74	Male	+	Cancer	Figures 1C, 1D, 1E and 1F
53	72	Male	+	Acute exacerbation of idiopathic pulmonary fibrosis	Figures 1D and 1E
54	74	Female	-	Intracerebral brain hemorrhage	Figures 1D and 1E

55	72	Male	-	Unknown	Figures 1D and 1E